Clinical Imaging 55 (2019) 29–34

Contents lists available at ScienceDirect

Clinical Imaging

journal homepage: www.elsevier.com/locate/clinimag

Neuroradiology

Pre-operative MRI predictors of hormonal remission status post pituitary adenoma resection

Maria Braileanu[a,*], Ranliang Hu[a], Michael J. Hoch[a], Mark E. Mullins[a], Adriana G. Ioachimescu[b,c], Nelson M. Oyesiku[c], Adlai Pappy II[d], Amit M. Saindane[a]

[a] Department of Radiology and Imaging Sciences, Emory University School of Medicine, 100 Woodruff Circle, Atlanta, GA 30322, United States of America
[b] Department of Medicine, Division of Endocrinology, Metabolism and Lipids, Emory University School of Medicine, 100 Woodruff Circle, Atlanta, GA 30322, United States of America
[c] Department of Neurosurgery, Emory University School of Medicine, 100 Woodruff Circle, Atlanta, GA 30322, United States of America
[d] Emory University School of Medicine, 100 Woodruff Circle, Atlanta, GA 30322, United States of America

ARTICLE INFO

Keywords:
Pituitary adenoma
Knosp score
CISS/FIESTA
VIBE/FAME/LAVA

ABSTRACT

Introduction: Contrast-enhanced (CE) Constructive Interference in Steady State (CISS) and Volumetric Interpolated Breath-hold Examination (VIBE) are MRI sequences used to improve the detection of pituitary adenomas and adjacent cranial nerves. The purpose of this study was to assess image quality and identify imaging predictors of postoperative hormonal remission of functioning pituitary adenomas using CE-T1 weighted image (WI), T2WI, CE-CISS, and CE-VIBE MRI sequences.

Materials and methods: Patients with pre-operative CE-T1WI, T2WI, CE-CISS, and CE-VIBE pituitary MRI sequences were included in this institutional retrospective review. Three raters independently reviewed randomized sequences in a blinded fashion for adenoma characteristics and parasellar invasion. Subgroup analysis of hormonal remission was performed.

Results: A total of 34 functioning pituitary adenoma patients were included (average age 39.3 ± 12.2; female n = 27), 30 of which had post-operative hormonal remission (n = 34; 88.2%). Compared to CE-T1WI, CE-CISS has significantly higher number of sequences rated "good" image quality ($p = 0.02$). Hormone remission was associated with decreased degrees of pre-operative internal carotid artery (ICA) contact and Knosp score ($p \leq 0.02$) on all sequences except for Knosp score on T2WI. On receiver operating characteristic analysis, the area under curve for differentiating endocrine remission ranged from 0.88 to 0.92 for Knosp score and 0.85–0.93 for ICA contact, depending on sequence.

Conclusion: Extent of pituitary adenoma cavernous sinus invasion as measured by degrees of ICA contact and Knosp score is associated with postoperative endocrine outcomes. Given improved image quality, inclusion of CE-CISS may be helpful for pre-surgical planning.

1. Introduction

Pituitary adenoma invasion of local structures on MRI is associated with postoperative outcomes following surgical resection [1–3]. The Knosp grade, used to evaluate pituitary tumor extension into the cavernous sinus on preoperative MRI, has been shown to be predictive of intraoperative tumor invasion, total resection, and postoperative hormonal remission [1,4]. Adenoma characteristics, such as size and invasion, are generally assessed using conventional MRI sequences, such as contrast-enhanced (CE) T1 weighted image (WI), and T2WI [1,3,4].

Newer MRI sequences, such as fully refocused steady-state gradient-echo sequences Fast Imaging Employing Steady-state Acquisition (FIESTA, GE Healthcare) and its counterpart Constructive Interference

Abbreviations: AUC, Area Under Curve; CE, Contrast Enhanced; CISS, Constructive Interference in Steady State; FIESTA, Fast Imaging Employing Steady-state Acquisition; ICA, Internal Carotid Artery; ICC, Intra-Class Correlation; ROC, Receiver Operating Characteristic; SE, Standard Error; VIBE, Volumetric Interpolated Breath-hold Examination; WI, Weighted Image

* Corresponding author at: 1364 Clifton Road NE, Atlanta, GA 30322, United States of America.
E-mail addresses: mbraile@emory.edu (M. Braileanu), ranliang.hu@emory.edu (R. Hu), michael.hoch@emory.edu (M.J. Hoch), memulli@emory.edu (M.E. Mullins), aioachi@emory.edu (A.G. Ioachimescu), noyesik@emory.edu (N.M. Oyesiku), adlai.pappy.ii@emory.edu (A. Pappy), asainda@emory.edu (A.M. Saindane).

https://doi.org/10.1016/j.clinimag.2019.01.020
Received 1 September 2018; Received in revised form 17 December 2018; Accepted 23 January 2019

in Steady State (CISS, Siemens Healthineers), and Volumetric Interpolated Breath-hold Examination (VIBE, Siemens Healthineers), have been used to improve the detection of pituitary adenomas and assess surrounding cranial nerves [5–13]. In the brain, FIESTA and CISS sequences (both hereon referred to as CISS for consistency) provides high spatial resolution, high fluid signal, and post-contrast enhancement of the cavernous sinus [5–7,11–13]. Similarly, VIBE can provide high spatial resolution, improved soft tissue contrast, and fat saturated imaging of the pituitary [8,9]. Following resection, CISS has been shown to be predictive of postoperative visual outcomes [5,6] and adenoma pathology [13].

Data on the use of CISS and VIBE for the assessment of postsurgical outcomes following pituitary adenoma resection is limited [5,6,13]. The purpose of this study was to assess image quality and identify imaging predictors of postoperative hormonal remission of functioning pituitary adenomas using conventional (CE- T1WI, T2WI) and newer (CE-CISS, CE-VIBE) MRI sequences.

2. Material and methods

2.1. Patient population and data collection

The study was approved by the local institutional review board and informed consent was exempted for this single institution retrospective chart review.

Imaging reports of patients diagnosed with hormonally-active pituitary adenomas who underwent transsphenoidal resection at our institution from 9/1/2010 to 9/1/2016 were retrospectively reviewed. Patients with pre-operative CE-T1WI, T2WI, and CE-CISS pituitary MRI imaging were included. Preoperative CE-VIBE imaging was also assessed but not required for inclusion. Patients with outside hospital preoperative imaging or prior pituitary surgery were excluded. All pituitary adenomas were resected by the same neurosurgeon at our institution (author N. M. O. – 1 year fellowship, 25 years of experience in neurosurgery). Patients were also listed in our institution's Pituitary Tumor Database that includes demographic, clinical, and biochemical characteristics for pituitary patients who underwent resection at our institution [14,15].

Baseline characteristics collected included age, and gender, as well as preoperative diagnosis with immunohistochemical confirmation of adenoma type, and short-term postsurgical hormonal outcomes. Short-term biochemical remission was defined at 3 months postoperatively based on the following criteria: 1) resolution of hypercortisolism for ACTH-secreting adenomas, 2) normalization of both IGF-1 and GH levels for GH-secreting adenomas, and 3) resolution of hyperprolactinemia for PRL-secreting adenomas.

2.2. MRI technique

As this was a retrospective clinical study, imaging was performed on a variety of MRI scanner types using similar but non-identical parameters. A standard dose (0.1 mmol/kg) of gadobenate dimeglumine (MultiHance, Bracco Diagnostics) was injected intravenously at 2–3 ml/s for all patients. Exams were performed on either a 1.5 T (n = 30; MAGNETOM Aera or Avanto, *Siemens Healthcare*) or a 3 T scanner (n = 4; MAGNETOM Trio, Siemens Healthcare) using a standard head coil. Typical parameters for 1.5 T coronal CE-T1WI: TE 15-17, TR 450-525, FOV 190 × 190, matrix 512 × 512, slice thickness 2–3 mm, and flip angle 90°. For 3 T coronal CE-T1WI: TE 9.7, TR 2130, FOV 172 × 200, matrix 276 × 320, slice thickness 2.5 mm, and flip angle 130°. For 1.5 T coronal T2WI: TE 77, TR 3304, FOV 185 × 185, matrix 512 × 512, slice thickness, 2.5 mm, and flip angle 150°. For 3 T coronal T2WI: TE 89, TR 3943–4570, FOV 199 × 199, matrix 384 × 384, slice thickness 2–2.5 mm, and flip angle 120°. For 1.5 T coronal CE-CISS: TE 2.45, TR 5.39, FOV 178 × 220, matrix 416 × 512, slice thickness 0.7 mm, and flip angle 62°. For 3 T coronal CE-CISS: TE 2.38, TR 5.27, FOV 195 × 240, matrix 416 × 512, slice thickness 0.7 mm, and flip angle 45°. For 1.5 coronal CE-VIBE: TE 3.76, TR 8.12, FOV 189 × 189, matrix 288 × 288, slice thickness 1.2 mm, and flip angle 10°. For 3 T coronal CE-VIBE: TE 3.25, TR 6.98, FOV 189 × 189, matrix 288 × 288, slice thickness 1.2 mm, and flip angle 10°.

2.3. Imaging analysis

For each patient, coronal CE-T1WI, T2WI, CE-CISS, and CE-VIBE sequences were collected and anonymized using OsiriX (Pixmeo SARL, Switzerland).

A list of traditionally assessed adenoma characteristics for each sequence was compiled. Characteristics included for evaluation were: image quality on all sequences (0 – poor, 1 – acceptable, 2 - good), heterogeneity of the lesion on CE-T1WI (0 – no, 1 – yes), cystic change on T2WI (0 – no, 1 – yes), bony invasion on CE-T1WI (0 – no, 1 – yes), suprasellar extension of lesion on CE-T1WI (0 – no, 1 – yes), mass effect on the optic chiasm on CE-CISS (0 – no, 1 – yes), mass effect on the third cranial nerve on CE-CISS (0 – no, 1 – yes), Knosp score on all sequences (0 – grade 0, 1 – grade 1, 2 – grade 2, 3 – grade 3a, 4 – grade 3b, 5 – grade 4), and degree of ICA contact on all sequences (0-360°). In addition, adenoma size (millimeters) in three dimensions (TRV, CC, AP) was obtained on CE-CISS, with the largest value used for final analysis.

The three raters independently reviewed the randomized unlabeled sequences on OsiriX. All raters were subspecialty board certified neuroradiologists (R. H. - 2-year neuroradiology fellowship, 2 years of neuroradiology experience; M. J. H. - 2-year neuroradiology fellowship, 2 years of neuroradiology experience; M. E. M. - 1-year neuroradiology fellowship, 14 years of neuroradiology experience). Participants were blind to post-surgical and clinical outcomes of the patient, and the responses of the other raters. For Knosp scoring, Fig. 1A from Micko et al., 2015 was provided for reference [1].

2.4. Statistical analysis

Responses of the three raters were compiled for further analysis, where median values of all three raters were used for categorical and ordinal variables, and mean values were used for continuous variables. Statistical analysis was performed using SPSS 24 (IBM Corp., Armonk, NY); cross-validation of ROC analysis was performed using STATA 14 (StataCorp., College Station, TX).

Intra-class correlation was used to assess interobserver reliability of all three raters using a two-way random average measure of absolute agreement. Agreement was defined as “excellent” for ICC values 0.75–1, “good” for 0.6–0.74, “fair” for 0.4–0.59, and “poor” for < 0.4 [16].

Subgroup analysis comparing patients with and without postoperative hormone remission was performed using chi-squared test for categorical values, and Mann-Whitney *U* test for ordinal and continuous variables. Nonparametric receiver operating characteristic (ROC) analysis was also conducted. Thresholds were based on optimal sensitivity and specificity. A p-value < 0.05 was defined as statistically significant. All p-values were reported as two sided.

3. Results

3.1. Patient characteristics

Of the 96 patients diagnosed with hormonally-active pituitary adenomas who underwent resection at our institution from 9/1/2010 to 9/1/2016 with preoperative MRI, 34 had CE-T1WI, T2WI, and CE-CISS MRI sequences performed at our institution. Of the 34 patients identified, 28 also had preoperative CE-VIBE imaging.

Average age was 39.3 ± 12.2 (n = 34) and the majority of patients were female (n = 27; 79.4%) (Table 1.1). Adenoma types included ACTH secreting tumor (n = 16; 47.1%), prolactinoma (n = 13, 38.2%),

Table 1.1
Subgroup analysis of post-surgical hormone remission status.

		Total	Remission	No remission	P
		n = 34 (%)	n = 30 (%)	n = 4 (%)	
Age	Years	39.3 ± 12.2	37.4 ± 9.9	53.3 ± 19.5	0.12
Gender	Female	27 (79.4)	25 (83.3)	2 (50)	0.12
	Male	7 (20.6)	5 (16.7)	2 (50)	
Adenoma type	ACTH	16 (47.1)	15 (50)	1 (25)	0.62
	GH	5 (14.7)	4 (13.3)	1 (25)	
	Prolactin	13 (38.2)	11 (36.7)	2 (50)	
CE-T1WI quality	Poor	5 (14.7)	3 (10)	2 (50)	
	Acceptable	12 (35.3)	11 (36.7)	1 (25)	0.10
	Good	17 (50)	16 (53.3)	1 (25)	
CE-T1WI heterogeneity	Yes	11 (32.4)	10 (33.3)	1 (25)	0.74
	No	23 (67.6)	20 (66.7)	3 (75)	
CE-T1WI bony invasion	Yes	5 (14.7)	5 (16.7)	0 (0)	0.38
	No	29 (85.3)	25 (83.3)	4 (100)	
CE-T1WI suprasellar extension	Yes	14 (41.2)	11 (36.7)	3 (75)	0.14
	No	20 (58.8)	19 (63.3)	1 (25)	
CE-T1WI ICA contact	(degrees)	73.6 ± 88.5	59.6 ± 80.1	179.2 ± 84.9	0.01*
CE-T1WI Knosp	0	18 (52.9)	18 (60)	0 (0)	0.005*
	1	7 (20.6)	7 (23.3)	0 (0)	
	2	6 (17.6)	3 (10)	3 (75)	
	3a	2 (5.9)	1 (3.3)	1 (25)	
	3b	0 (0)	0 (0)	0 (0)	
	4	1 (2.9)	1 (3.3)	0 (0)	
T2WI quality	Poor	3 (8.8)	3 (10)	0 (0)	0.15
	Acceptable	11 (32.4)	8 (26.7)	3 (75)	
	Good	20 (58.8)	19 (63.3)	1 (25)	
T2 cystic	Yes	14 (41.2)	12 (40)	2 (50)	0.70
	No	20 (58.8)	18 (60)	2 (50)	
T2WI ICA contact	(degrees)	76.8 ± 90.0	62.6 ± 79.5	182.9 ± 104.5	0.02*
T2WI knosp	0	16 (47.1)	15 (50)	1 (25)	0.15
	1	10 (29.4)	9 (30)	1 (25)	
	2	5 (14.7)	5 (16.7)	0 (0)	
	3a	1 (2.9)	0 (0)	1 (25)	
	3b	1 (2.9)	0 (0)	1 (25)	
	4	1 (2.9)	1 (3.3)	0 (0)	
CE-CISS quality	Poor	1 (2.9)	1 (3.3)	0 (0)	0.29
	Acceptable	7 (20.6)	5 (16.7)	2 (50)	
	Good	26 (76.5)	24 (80)	2 (50)	
CE-CISS mass effect chiasm	Yes	6 (17.6)	5 (16.7)	1 (25)	0.68
	No	28 (82.4)	25 (83.3)	3 (75)	
CE-CISS mass effect cranial nerve III	Yes	2 (5.9)	2 (6.7)	0 (0)	0.60
	No	32 (94.1)	28 (93.3)	4 (100)	
CE-CISS SIZE	(mm)	14.7 ± 9.9	14.2 ± 10.0	18.5 ± 9.0	0.34
CE-CISS ICA contact	(degrees)	81.1 ± 84.4	68.1 ± 79.3	178.3 ± 57.3	0.01*
CE-CISS Knosp	0	18 (52.9)	18 (60)	0 (0)	0.009*
	1	8 (23.5)	7 (23.3)	1 (25)	
	2	2 (5.9)	2 (6.7)	0 (0)	
	3a	3 (8.8)	1 (3.3)	2 (50)	
	3b	2 (5.9)	1 (3.3)	1 (25)	
	4	1 (2.9)	1 (3.3)	0 (0)	

		Total	Remission	No remission	P
		n = 28 (%)	n = 25(%)	n = 3 (%)	
CE-VIBE quality (n = 28)	Poor	3 (10.7)	2 (8)	1 (33.3)	0.23
	Acceptable	10 (35.7)	10 (40)	0 (0)	
	Good	15 (53.6)	13 (52)	2 (66.7)	
CE-VIBE ICA contact (N = 28)	(degrees)	87.6 ± 92.0	72.1 ± 81.5	216.7 ± 80.2	0.02*
CE-VIBE knosp (N = 28)	0	13 (46.4)	13 (52)	0 (0)	0.01*
	1	8 (28.6)	8 (32)	0 (0)	
	2	3 (10.7)	2 (8)	1 (33.3)	
	3a	3 (10.7)	1 (4)	2 (66.7)	
	3b	0 (0)	0 (0)	0 (0)	
	4	1 (3.6)	1 (4)	0 (0)	

ACTH = ACTH secreting tumor, GH = Growth hormone secreting tumor, Prolactin = Prolactinoma.
* Statistically significant.

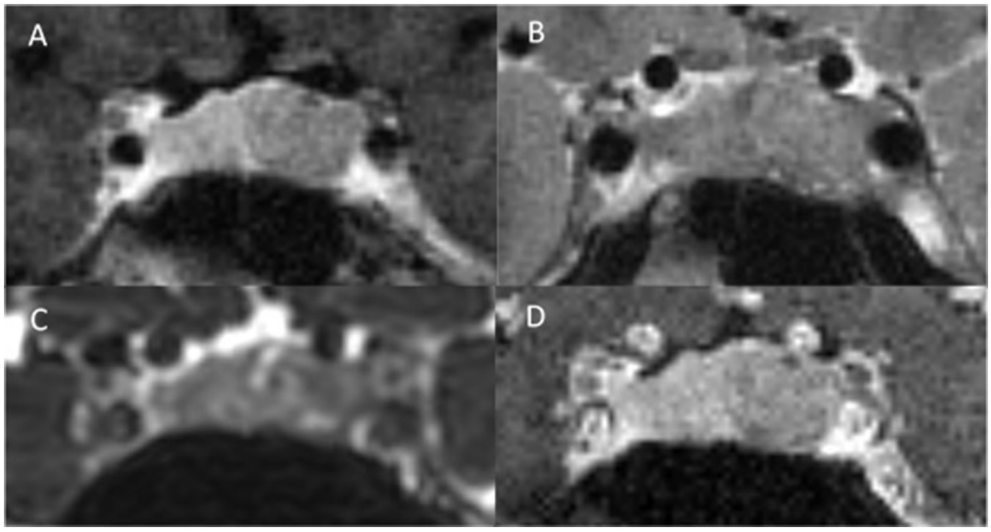

Fig. 1.1. A pituitary prolactinoma that extends into the left cavernous sinus rated as Knosp grade (A) 2 on CE-T1WI, (B) 1 on T2WI, (C) 3a on CE-CISS, and (D) 2 on CE-VIBE. This patient did not have endocrine remission after resection.

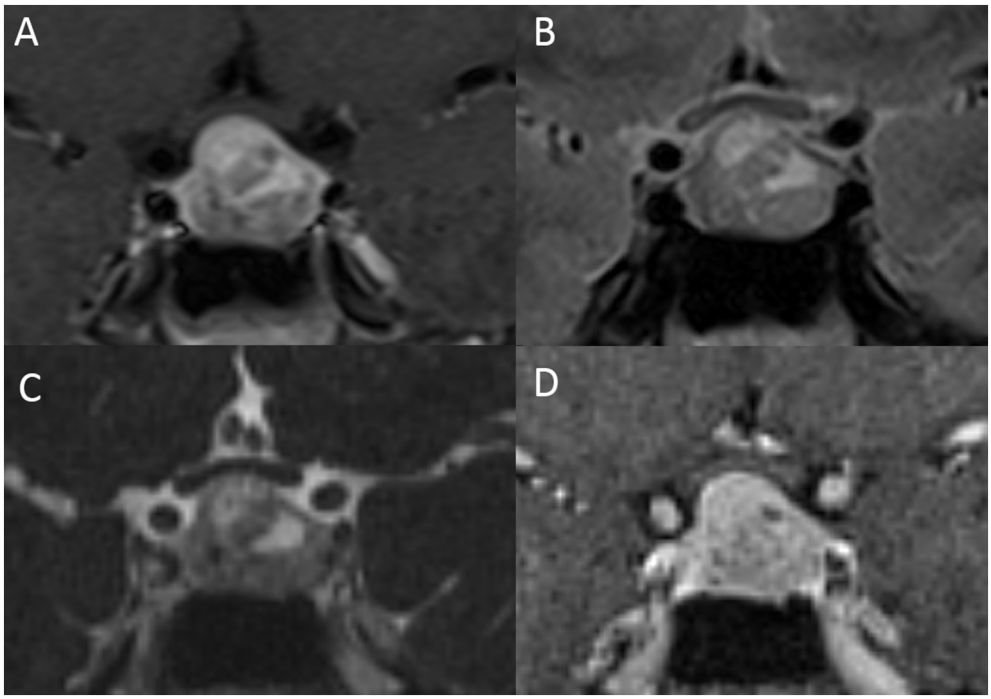

Fig. 2.1. A partially cystic pituitary prolactinoma rated as Knosp grade 1 on (A) CE-T1WI, (B) T2WI, (C) CE-CISS, and (D) CE-VIBE. This patient did have endocrine remission after resection.

and growth hormone secreting tumor (n = 5; 14.7%). The increased number of ACTH secreting tumors relative to prolactinomas was expected in this surgical group, as the latter is often treated medically as first line therapy. Post-operative hormone remission was observed in 30 patients (n = 34; 88.2%) (Table 1.1, Fig. 1.1 & 2.1).

3.2. Image analysis

A total of 130 imaging sequences were analyzed in random order by three raters blinded to patient identity and clinical outcomes. Summary results for all patients, divided into subgroups based on remission status, are included in Table 1.1. Baseline characteristics (age, gender, and tumor type) did not differ significantly between the two groups.

On quality scoring, CE-CISS had the fewest number of sequences rated “poor” (n = 1, 2.9%) while CE-T1WI had the highest (n = 5, 14.7%). Contrast enhanced CISS had the highest number of sequences rated “good” (n = 26, 76.5%), while CE-VIBE (n = 15, 53.6%) and CE-T1WI had the lowest (n = 17, 50.0%). The difference in “good” rating was significantly different between CE-T1WI and CE-CISS (p = 0.02) (Fig. 3.1).

3.3. Subgroup analysis

Knosp score and degree of ICA contact correlated with post-operative remission status. Knosp score was significantly lower in patients with hormonal remission on all sequences (CE-T1WI, p = 0.005; CE-CISS, p = 0.009; CE-VIBE, p = 0.01) except T2WI (p = 0.15). The average degree of ICA contact was higher and significantly different for

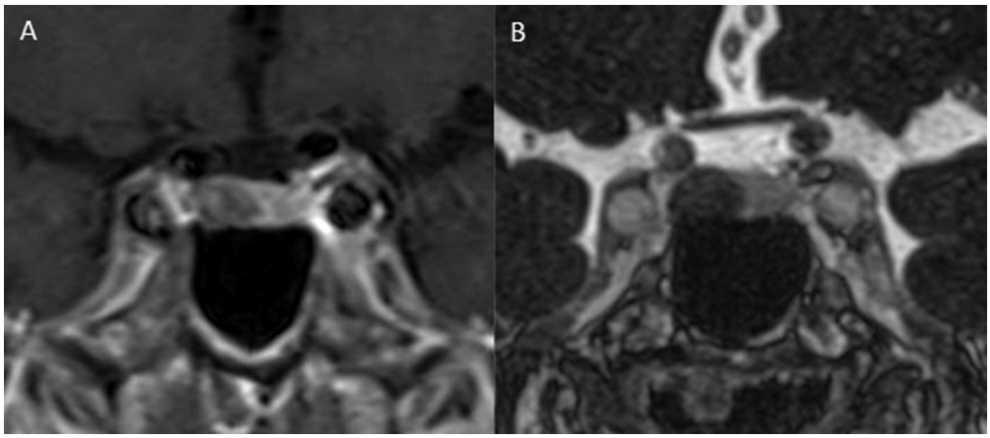

Fig. 3.1. Knosp grade 0 ACTH secreting tumor with median agreement of (A) "acceptable" on CE-T1WI and (B) "good" on CE-CISS sequences. Higher spatial resolution and contrast between tumor and background is demonstrated on CE-CISS sequences. Significantly more CE-CISS sequences were rated "good" compared to CE-T1WI.

patients without hormonal remission, compared to patients with, on all MRI sequences (CE-T1WI, p = 0.01; T2WI, p = 0.02; CE-CISS, p = 0.01; CE-VIBE, p = 0.02). Other characteristics including maximum size on CISS, mass effect on the optic chiasm or third cranial nerve on CE-CISS, suprasellar extension or bony invasion on CE-T1WI, and cystic changes on T2WI were not significantly associated with postoperative hormonal remission status.

3.4. ROC analysis

For differentiating endocrine remission, average degree of ICA contact on CE-T1 W1, T2WI, CE-CISS, and CE-VIBE, and Knosp score on CE-T1WI, CE-CISS, and CE-VIBE were assessed through ROC analysis (Table 2.1). The area under the curve (AUC) for Knosp score ranged from 0.88 (Standard Error (SE) 0.07, 95%CI[0.74–1.0]) on CE-CISS to 0.92 (SE 0.05, 95%CI[0.82–1.0]) on CE-VIBE. Threshold value of Knosp score 2 on CE-VIBE resulted in a sensitivity, specificity, and accuracy of 100%, 84%, and 85.7%, respectively. Average degree of ICA contract in differentiating endocrine remission resulted in AUC ranging from 0.85 (SE 0.10, 95%CI[0.66–1.0]) on T2WI to 0.93 (SE 0.05, 95%CI [0.83–1.0]) on CE-VIBE. At a threshold of 140 degrees on CE-VIBE, sensitivity was 100%, specificity 88%, and accuracy 89.3%.

3.5. Inter-observer agreement

Inter rater reliability (Table 3.1) ranged from excellent for mass effect on the chiasm on CE-CISS sequences (ICC = 0.95, 95%[0.92–0.97], p < 0.001), to fair for bone invasion on CE-T1WI (ICC = 0.48, 95%[0.12–0.72], p = 0.002). Agreement was excellent on all sequences for degree of ICA involvement and Knosp score.

4. Discussion

In this study, traditionally assessed pituitary adenoma characteristics were analyzed using both conventional (CE-T1WI, T2WI), and newer (CE-CISS, CE-VIBE) MRI sequences. Pituitary adenoma cavernous invasion, as measured by increasing Knosp score and degrees of ICA contact, was shown to be inversely associated with post-surgical hormonal remission on CE-T1WI, T2WI (ICA contact only), CE-CISS, and CE-VIBE sequences. These findings are in accordance to prior studies which utilized traditional MRI sequences to assess pituitary adenoma parasellar extension [1–3]. Our results suggest assessment of pituitary adenoma extension on newer MRI sequences such as CE-CISS and CE-VIBE is also predictive of post-operative hormonal outcomes.

Our findings suggest CE-CISS and CE-VIBE may also be useful in predicting hormonal outcomes in pre-operative planning of pituitary adenoma resection. Prior studies have shown the predictive value of

Table 3.1
Interrater reliability of traditionally assessed pituitary adenoma characteristics.

	ICC	p	95% CI
CE-T1WI quality	0.71	< 0.001	0.29–0.87
CE-T1WI heterogeneity	0.63	< 0.001	0.34–0.80
CE-T1WI bony invasion	0.48	0.002	0.12–0.72
CE-T1WI suprasellar extension	0.73	< 0.001	0.53–0.86
CE-T1WI ICA contact	0.90	< 0.001	0.81–0.95
CE-T1WI knosp	0.89	< 0.001	0.80–0.95
T2WI quality	0.76	< 0.001	0.58–0.87
T2WI cystic	0.76	< 0.001	0.54–0.87
T2WI ICA contact	0.89	< 0.001	0.79–0.94
T2WI knosp	0.87	< 0.001	0.77–0.93
CE-CISS quality	0.70	< 0.001	0.48–0.84
CE-CISS mass effect chiasm	0.95	< 0.001	0.92–0.97
CE-CISS mass effect cranial nerve III	0.75	< 0.001	0.56–0.87
CE-CISS SIZE	0.84	< 0.001	0.70–0.92
CE-CISS ICA contact	0.92	< 0.001	0.82–0.96
CE-CISS knosp	0.88	< 0.001	0.77–0.94
CE-VIBE quality	0.80	< 0.001	0.62–0.90
CE-VIBE ICA contact	0.92	< 0.001	0.83–0.96
CE-VIBE knosp	0.90	< 0.001	0.81–0.95

95%CI = 95% Confidence Interval, ICC = Intra-Class Correlation.

Table 2.1
Receiver operating curve analysis for predicting post-surgical hormone remission status using Knosp grade and degree of ICA contact on various sequences.

	N	AUC	SE	95%CI	Threshold	Sensitivity	Specificity	Accuracy
CE-T1WI ICA contact	34	0.88	0.06	0.76–1.0	120°	100%	80%	82.4%
CE-T1WI Knosp	34	0.90	0.05	0.80–1.0	2*	100%	83.3%	85.3%
T2WI ICA contact	34	0.85	0.10	0.66–1.0	141.6°	75%	86.7%	85.3%
CE-CISS ICA contact	34	0.89	0.06	0.77–1.0	150°	75%	83.3%	82.4%
CE-CISS knosp	34	0.88	0.07	0.74–1.0	3*	75%	90%	88.2%
CE-VIBE ICA contact	28	0.93	0.05	0.83–1.0	140°	100%	88%	89.3%
CE-VIBE knosp	28	0.92	0.05	0.82–1.0	2*	100%	84%	85.7%

95%CI = 95% Confidence Interval, AUC = Area Under Curve, ROC = Receiver Operating Characteristic, SE = Standard Error.
* Knosp score on all sequences: 0 – grade 0, 1 – grade 1, 2 – grade 2, 3 – grade 3a, 4 – grade 3b, 5 – grade 4.

Knosp grading using traditional MRI sequences without comparing between sequences [1,4]. Micko and colleagues assessed Knosp score on coronal pre- and post-contrast T1WI; T2WI was included in most cases [1]. Our study demonstrates extent of pituitary adenoma cavernous sinus invasion, as measured by Knosp score, was associated with hormonal outcome on every sequence except T2WI. Furthermore, CE-VIBE has the largest AUC for both ICA contact (AUC = 0.92) and Knosp score (AUC = 0.93) with high to moderate sensitivity, specificity, and accuracy at a threshold values of 140 degrees and Knosp score of 2. The predictive value of CE-CISS was similar to T1WI. Contrast enhanced CISS and VIBE sequences may supplement traditional sequences, such as T2WI and post-contrast T1WI, when assessing pituitary adenoma parasellar extension.

In addition, by providing improved resolution of the sella and surrounding structures [5–9,11–13], CE- CISS sequences may augment the pre-operative assessment of pituitary adenomas. In our study, CE-CISS had a significantly ($p = 0.02$) higher percentage of sequences rated "good" (76.5%) compared to T1WI (50.0%). Prior studies have shown significantly increased visibility of the optic pathways on FIESTA (CISS) relative to conventional imaging [5,6]. In addition, prior studies have found VIBE to be rated superior to T1WI in cavernous sinus contrast enhancement and anatomic assessment [8]. Our results suggest CE-CISS sequences may augment pre-operative assessments relative to traditional sequences through improved image quality.

Interrater reliable assessment of pituitary adenomas on newer (CE-CISS, CE-VIBE) MRI sequences is akin to conventional CE-T1WI and T2WI, with prior reports focusing on adenoma detection on conventional sequences. De Rotte and colleagues reported "good" Kappa agreement on the detection of pituitary lesions in patients with Cushing's disease using 1.5 T MRI, specifically, pre- and post-contrast T1WI TSE and T2WI TSE for all patients, and dynamic T1WI TSE for most patients [17]. Additionally, Tabarin and co-authors demonstrated "very good" kappa agreement on the detection of ACTH-secreting adenomas on non-contrast spin-echo T1WI and T2WI TSE, as well as CE spin-echo T1WI [18]. Excellent interrater reliability of the Knosp score using Spearman correlation coefficient on presumed traditional MRI sequences of pituitary adenomas has been reported [4]. In the current study, interrater reliability of the Knosp scale and ICA contact was excellent for CE-T1 W1, T2 W1, CE-VIBE, and CE-CISS MRI sequences.

There are several limitations of this study. First, the overall number of patients without hormonal remission after resection was small. Although statistically significant imaging predictors of hormone remission were found, comparison between individual sequences and characteristics was limited by power. Next, the study was retrospective, and images were obtained from over six years and inevitably varied in quality. However, < 10% of images were deemed "poor" quality by the raters (n = 12 of 130 sequences). Finally, at this time long term follow-up was not available on all patients and our analysis was limited to short-term post-operative hormonal outcome. Future prospective research with a larger number of patients may focus on predictors of long term remission versus reoccurrence.

5. Conclusions

Pituitary adenoma cavernous sinus invasion, as measured by degrees of ICA contact and Knosp score on CE-CISS, and CE-VIBE MRI sequences, is associated with postoperative endocrine outcomes. The predictive value and interrater reliability of CE-CISS is similar to CE-T1WI. However, a significantly higher percentage of CE-CISS sequences had a higher quality rating compared to CE-T1WI, in agreement with prior studies demonstrating improved anatomical delineation of the sella on CISS. Given improved image quality and significant Knosp scoring relative to traditional sequences, especially T2WI, inclusion of CE-VIBE and CE-CISS MRI sequences may augment pre-surgical planning of adenoma resection.

Funding

This research did not receive any specific grant from funding agencies in the public, commercial, or not-for-profit sectors.

References

[1] Micko ASG, Wöhrer A, Wolfsberger S, Knosp E. Invasion of the cavernous sinus space in pituitary adenomas: endoscopic verification and its correlation with an MRI-based classification. J Neurosurg 2015;122:803–11. https://doi.org/10.3171/2014.12.JNS141083.

[2] Brochier S, Galland F, Kujas M, Parker F, Gaillard S, Raftopoulos C, et al. Factors predicting relapse of nonfunctioning pituitary macroadenomas after neurosurgery: a study of 142 patients. Eur J Endocrinol 2010;163:193–200. https://doi.org/10.1530/EJE-10-0255.

[3] Sanmillán JL, Torres-Diaz A, Sanchez-Fernández JJ, Lau R, Ciller C, Puyalto P, et al. Radiological predictors for extent of resection in pituitary adenoma surgery. A single-center study. World Neurosurg 2017:436–46. https://doi.org/10.1016/j.wneu.2017.09.017.

[4] Mooney MA, Hardesty DA, Sheehy JP, Bird R, Chapple K, White WL, et al. Interrater and intrarater reliability of the Knosp scale for pituitary adenoma grading. J Neurosurg 2016;126:1714–9. https://doi.org/10.3171/2016.3.JNS153044.

[5] Hisanaga S, Kakeda S, Yamamoto J, Watanabe K, Moriya J, Nagata T, et al. Pituitary macroadenoma and visual impairment: postoperative outcome prediction with contrast-enhanced FIESTA. AJNR Am J Neuroradiol 2017. https://doi.org/10.3174/ajnr.A5394.

[6] Watanabe K, Kakeda S, Yamamoto J, Watanabe R, Nishimura J, Ohnari N, et al. Delineation of optic nerves and chiasm in close proximity to large Suprasellar tumors with contrast-enhanced FIESTA MR imaging. Radiology 2012;264:852–8. https://doi.org/10.1148/radiol.12111363.

[7] Amemiya S, Aoki S, Ohtomo K. Cranial nerve assessment in cavernous sinus tumors with contrast-enhanced 3D fast-imaging employing steady-state acquisition MR imaging. Neuroradiology 2009;51:467–70. https://doi.org/10.1007/s00234-009-0513-z.

[8] Davis MA, Castillo M. Evaluation of the pituitary gland using magnetic resonance imaging: T1-weighted vs. VIBE imaging. Neuroradiol J 2013;26:297–300.

[9] Grober Y, Grober H, Wintermark M, Jane JA, Oldfield EH. Comparison of MRI techniques for detecting microadenomas in Cushing's disease. J Neurosurg 2017:1–7. https://doi.org/10.3171/2017.3.JNS163122.

[10] Ma J, Su S, Yue S, Zhao Y, Li Y, Chen X, et al. Preoperative visualization of cranial nerves in Skull Base tumor surgery using diffusion tensor imaging technology. Turk Neurosurg 2016;26:805–12. https://doi.org/10.5137/1019-5149.JTN.13655-14.1.

[11] Tong T, Yue W, Zhong Y, Zhenwei Y, Yong H, Xiaoyuan F. Comparison of contrast-enhanced SPACE and CISS in evaluating cavernous sinus invasion by pituitary macroadenomas on 3-T magnetic resonance. J Comput Assist Tomogr 2015;39:222–7. https://doi.org/10.1097/rct.0000000000000191.

[12] Xie T, Zhang XB, Yun H, Hu F, Yu Y, Gu Y. 3D-FIESTA MR images are useful in the evaluation of the endoscopic expanded endonasal approach for midline skull-base lesions. Acta Neurochir 2011;153:12–8. https://doi.org/10.1007/s00701-010-0852-x.

[13] Yamamoto J, Kakeda S, Shimajiri S, Takahashi M, Watanabe K, Kai Y, et al. Tumor consistency of pituitary macroadenomas: predictive analysis on the basis of imaging features with contrast-enhanced 3D FIESTA at 3T. Am J Neuroradiol 2014;35:297–303. https://doi.org/10.3174/ajnr.A3667.

[14] Anthony JR, Alwahab UA, Kanakiya NK, Pontell DM, Veledar E, Oyesiku NM, et al. Significant elevation of growth hormone level impacts surgical outcomes in acromegaly. Endocr Pract 2015;21:1001–9. https://doi.org/10.4158/EP14587.OR.

[15] Tindall GT, Oyesiku NM, Watts NB, Clark RV, Christy JH, Adams DA. Transsphenoidal adenomectomy for growth hormone-secreting pituitary adenomas in acromegaly: outcome analysis and determinants of failure. J Neurosurg 1993;78:205–15. https://doi.org/10.3171/jns.1993.78.2.0205.

[16] Hallgren KA. Computing inter-rater reliability for observational data: an overview and tutorial. Tutor Quant Methods Psychol 2012;8:23–34.

[17] de Rotte AAJ, Groenewegen A, Rutgers DR, Witkamp T, Zelissen PMJ, Meijer FJA, et al. High resolution pituitary gland MRI at 7.0 Tesla: a clinical evaluation in Cushing's disease. Eur Radiol 2016;26:271–7. https://doi.org/10.1007/s00330-015-3809-x.

[18] Tabarin A, Laurent F, Catargi B, Olivier-Puel F, Lescene R, Berge J, et al. Comparative evaluation of conventional and dynamic magnetic resonance imaging of the pituitary gland for the diagnosis of Cushing's disease. Clin Endocrinol (Oxf) 1998;49:293–300. https://doi.org/10.1046/j.1365-2265.1998.00541.x.